UNIVERSITY OF CALIFORNIA, SAN DIEGO

Design of Bone Morphogenetic Protein 2/Nodal Chimeras

A Thesis submitted in partial satisfaction of the requirement for the degree
Master of Science

in

Biology

by

Alissa N. Blackler

Committee in charge:

Professor Senyon Choe, Chair
Professor Colin Jamora, Co-Chair
Professor Yang Xu

2010

ProQuest LLC
789 East Eisenhower Parkway
P.O. Box 1346
Ann Arbor, MI 48106-1346

The Thesis of Alissa N. Blackler is approved, and is accepted in quality and form for publication on microfilm and electronically:

_____

_____

Co-Chair

_____

Chair

University of California, San Diego

2010

TABLE OF CONTENTS

LIST OF FIGURES

LIST OF TABLES

ACKNOWLEDGEMENTS

I would like to thank my graduate advisor, Senyon Choe, for his continued support during my Master's Degree program.

I would like to thank my colleague and Post-doc, George Allendorph, for his support and guidance in the lab.

I would like to thank our collaborator, Peter Gray from the Peptide Biology Laboratory at the Salk Institute for his help with cell based assays.

This Thesis, in part, is being prepared for publication of the material as it may appear as Blackler, Alissa N., Allendorph, George P., Choe, Senyon, Gray, Peter 2010. The thesis author will be the primary investigator and author of this paper.

ABSTRACT OF THE THESIS

Design of Bone Morphogenetic Protein 2/Nodal Chimeras

by

Alissa N. Blackler

Master of Science in Biology

University of California, San Diego, 2010

Professor Senyon Choe, Chair
Professor Colin Jamora, Co-Chair

The TGF-β superfamily is comprised of over thirty ligands responsible for numerous cellular processes including early embryonic development, tissue patterning and homeostasis, bone formation, wound healing and fibrosis. Research is directed at utilizing these ligands as protein-based therapies. Bone Morphogenetic Protein 2 (BMP-2) is currently used to facilitate fracture repair and spinal fusions. In order to sustain

these efforts, *E. Coli* derived, chemically refolded ligands provide an efficient, cost effective alternative to using stably transfected cell lines. Currently, less than a dozen of the TGF-β ligands have been successfully refolded. The aim of my project was to create chimeric proteins by recombining a ligand that refolds well with a non-refolding ligand. Nodal, an essential TGF-β ligand responsible for axis formation in early embryonic development, was recombined with BMP-2, a ligand known for its efficient refolding. Using our strategy, we successfully generated multiple ligands with Cripto-dependent signaling comparable to wild type Nodal. Based on our findings, we were able to identify a region within Nodal's structure that is critical for Cripto-dependent signaling. We will use our chimeras to better understand receptor ligand compelx formation and its modulation of intracellular downstream signaling.

Introduction:

In 1978, while studying the transformation of normal cells into cancer cells, De Larco and Todaro were able to create anchorage-independent growth associated with transformed cells (De Larco and Todaro 1987). They coined the term "transforming growth factors" (TGFs) and outlined a partial purification of the polypeptide growth factors isolated from fibroblasts (De Larco and Todaro 1978). Following their work, two papers in 1981 conducted in Harold Moses' lab and Michaels Spron's lab further explored and isolated factors known today as TGF-β (Moses et al. 1981, Roberts et al 1981). These initial discoveries sparked interest in these potentially powerful factors, leading to the discovery of close to forty related growth factors known to have profound effects on embryonic development, tissue differentiation and proliferation, maintenance of pluripotency, tissue homeostasis in adults, and numerous diseases including wound healing, fibrosis, and carcinogenesis.

Conserved Structural Similarity of TGF-β Superfamily

The different known growth factors within the TGF-β Superfamily share similar sequence structure. Early research of transforming growth factors revealed differences in cDNA sequences, differentiating TGF-β1 from TGF-α. It was then found that the carboxy terminal of a much larger precursor served as the starting material for what eventually was proteolytically cleaved to form the mature TGF-β monomer. Soon after, heterodimer disulfide-linked inhibin was shown to be structurally related to TGF-β, and

also possessed the carboxy terminal of the larger precursor, which led people to believe that a superfamily might exist (Mason et al., 1985, Vale et al. 1986). The known mammalian TGF-β family consists of thirty three genes which encode secreted proteins with an amino terminal signal peptide thought to regulate the release and presentation of the mature protein, a large precursor segment or prosegment thought to act as a chaperone and possibly interact with latent TGF-β binding proteins to mediate targeting of TGF-β proteins, and a carboxy terminal TGF-β family monomer.

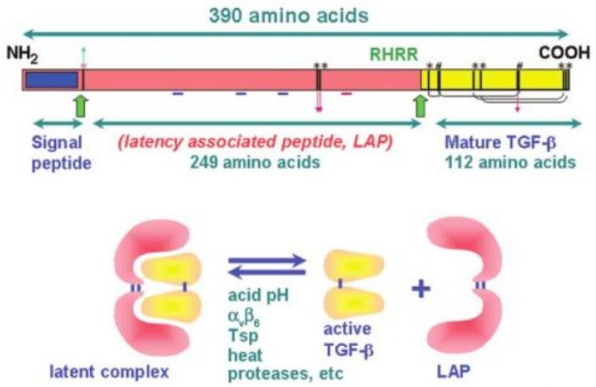

Figure 1: Conserved Structural Architecture of TGF-β Superfamily. This figure shows the conserved structural architecture of the TGF-β superfamily. The ligands consist of an amino terminal signal peptide, the prodomain, and the mature TGF-β ligand at the carboxy terminal (Derynck et al 2008).

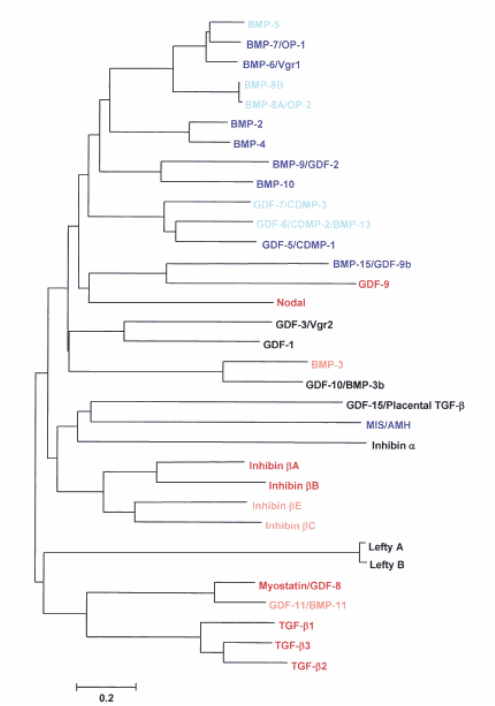

Figure 2: Phylogenetic tree of TGF-β ligands in humans. The evolutionary relationships were determined by ClustalW amino acid sequence alignment (Derynck et al 2008). Ligands that activate TGF-β/activin-type Smads are shown in red while ligands that activate BMP-type Smads are in blue.

Within the TGF-β family, subfamilies exist with different numbers and locations of cysteines. The spacing and conservation of the cysteines are an integral part of what make the TGF-β family unique, allowing formation of covalently disulfide-linked dimers. TGF-β ligands TGF-β 1, TGF-β 2 and TGF-β 3 are part of their own subfamily with nine aligned cysteins and a single intramolecular disulfide bridge resulting in dimer formation (Daopin et al. 1992, Schlunegger and Grutter 1992). The inhibin-β family consists of herterodimers containing an inhibin-β chain with 9 cysteins similar to the TGF-βs, and an inhibin-α chain with seven cysteins in the carboxy terminal. In all but

five of the rest of the proteins in the family, there are seven cysteins, with the fourth cystein responsible for dimerization. Lefty A, lefty B, BMP-15, GDF-9 and GDF-3 only possess six cysteines, lacking the fourth cystein responsible for dimerization. They have been found to associate and inhibit some of the other family members while interacting with Smad signaling molecules (Chen Shen 2004; Tabibzadeh and Hemmati-Brivanlou 2006, Moore et al. 2003; Mazerbourg et al. 2004). Within each molecule, 6 of the cysteines form intradisulfide bonds, creating the 'cystein knot' motif (McDonald and Hendrickson 1993). The similarities in sequences among the TGF-β family result in similarities in three dimensional structure. The TGF-β family members are typically thought to form butterfly-like homodimers, but are also known to associate in a heterodimeric complex.

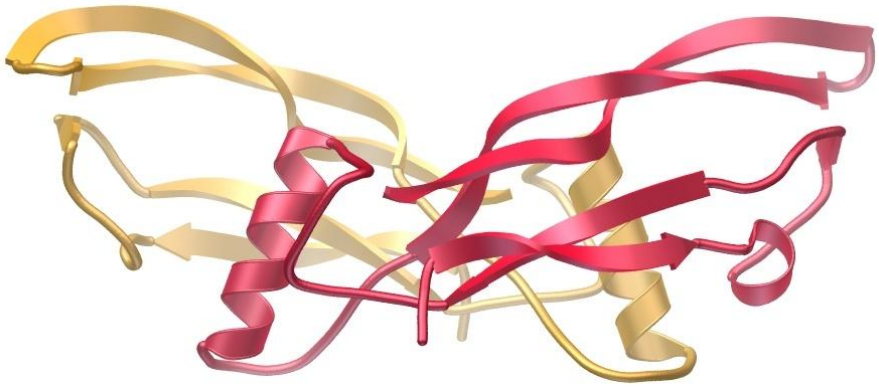

Figure 3: Ribbon diagram of dimeric TGF-β ligand in butterfly conformation.

Signaling

TGF-β family members signal through a number of cell surface, serine and threonine kinase transmembrane receptors. These are broken into Type I and Type II receptors. At the cell surface, complexes form once a ligand associates with two Type II receptors and two Type I receptors. Type I receptors have a glycine serine rich sequence

upstream of the kinase domian that is phosphorylated by Type II receptors, activating the Type I receptor. In humans, seven Type I receptors and five Type II receptors have been identified. Upon activation by a ligand, a conformational change occurs, allowing different heteromeric receptor complexes to initiate signaling. Also important in TGF-β signaling, Smads are known to be directly phosphorylated by Type I receptors. The complexes formed have been shown to migrate to the nucleus, regulating transcription processes. Of the eight known Smads in mammals, Smad2 and Smad3 are activated by activins, myostatin, and Nodal. They then form hetero-oligomerica complexes with the common mediator (co-) Smad (Smad 4 in humans). Smad1, Smad5 and Smad8 are activated by BMPs, GDFs and MIS. One of the best understood mechanisms for regulation of TGF-β signaling is through extracellular agonists and antagonists. While some disrupt or prevent the binding of TGF-β ligands to their receptors, others aid in maturation, or enhance binding and amplification of their signal. Cell-surface proteoglycans interact with both TGF-β ligands and their regulators, affecting downstream signaling events.

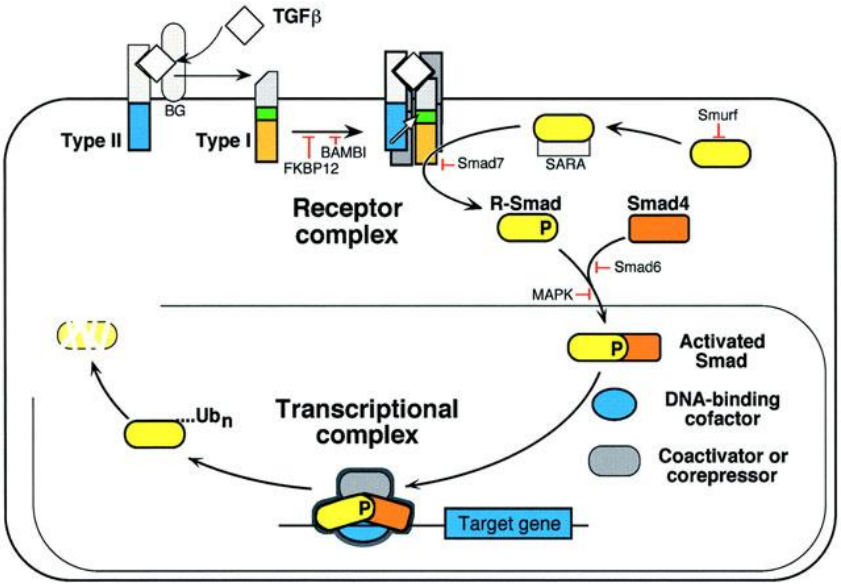

Figure 4: TGF-β signal transduction. Interaction with Type I and Type II receptors leads to the activation of Smads and eventually alters transcription (Massague 2000).

Bone Morphogenetic Proteins

Urist's use of implanted demineralized bone matrix at intramuscular sites in 1965 lead to the discovery of "bone morphogenetic proteins (BMPs)" (Urist 1965). Since then, over twenty BMPs have been discovered in vertebrates and invertebrates. They are essential in embryonic development. Both intramembranous and endochondral ossification allow formation of skeletal tissue and are strongly influenced by BMPs. In addition to contributions to bone and cartilage development, BMPs are important to hair, kidney, tooth and neural cell development while inhibiting myogenesis. Excluding BMP-1, the BMPs have highly conserved structures. The BMP subfamily is further broken down into smaller groupings. BMP-2 and BMP-4 are highly similar and form a subgroup within the homologous BMPs. Signaling for BMPs involves different receptors. BMPRIA (ALK-3), BMPRIB (ALK-6), most commonly act as Type I receptors (ALK-2,

and ALK-1 have been implicated as serving as Type I receptors, but are less commonly associated), while BMPRII, ActRII and ActRIIB function as Type II receptors. BMP-2 is generally thought to have higher affinity for Type I receptors. The binding profiles to Type I receptors of BMPs tend to show differences based on the tissue type they are found in and are affected by type II receptors (Yu et al. 2005). Because of its ability to stimulate bone and cartilage growth, researchers have used recombinant human BMP-2 in combination with absorbable collagen sponge (ACS) therapeutically to treat fracture repair and spinal fusions (Geiger 2003).

Nodal

Discovered based on a lack of early mesoderm and primitive streak markers due to a retroviral insertion, Nodal is known to be essential in embryonic development (Zhou et al. 1993; Conlon et al. 1994). Nodal has been shown to be critical in mesoderm development and its complex interactions with embryonic and extraembryonic tissues leaves room for further investigation (Schier and Shen 2000; Whitman and Mercola 2001; Schier 2003). While it is unclear how Nodal expression is initiated, it is present very early on in the epiblast and visceral endoderm (Zhou et al. 1993). Preceding gastrulation, Nodal expression is localized in the proximal posterior region of the embryo, with its' highest concentration in the developing primitive streak. Nodal expression is then concentrated in the node through the end of gastrulation. Nodal's asymmetric expression leads to proximal-distal patterning and anterior-posterior patterning before gastrulation. This patterning leads to the asymmetry very essential for development and necessary for life. Studies show that Type II receptors ActRII and

ActRIIB and Type I receptor ALK-4 (ActRIB) are integral in Nodal signaling (Gu et al. 1998; Song et al 1999). Nodal strongly associates with its Type II receptor and does not show Type I receptor binding without Type II receptor present. One unique feature is Nodal's dependence on the extracellular membrane-anchored coreceptor Cripto for signaling (Schier and Shen 2000; Whitman 2001; Schier 2003). Interestingly, Cripto inhibits activin's signaling.

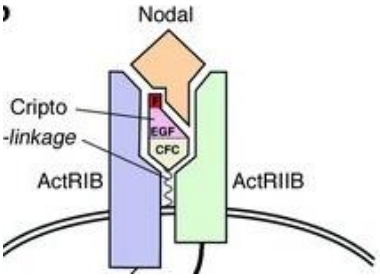

Figure 5: Representation of Cripto dependence of Nodal (Shen 2003).

TGF-β Ligand Refolding and Chimeras

In order for the TGF-β ligands to perform the proper function within the cell, they must be properly folded. Failure to fold properly results in inactive proteins which often times aggregate. In human cells, most of these ligands are folded with the aid of chaperones along with particular concentrations of salts and a specific pH and temperature within the cell. Due to the low yield of properly folded protein that can be extracted from human cells, researchers have turned to chemical refolding as an alternative. Chemical refolding has been shown to be fast and efficient while producing large yields. In 1998, Groppe was able to successfully chemically refold Drosophila Decapentaplegic proprotein by isolating inclusion bodies followed by heparin affinity chromatography and reverse phase HPLC (Groppe 1998). They were able to

purify 3mg of protein per liter of bacterial growth (Groppe 1998). Chemically refolded proteins that are often difficult to refold can be expressed in *Escherichia Coli*. The bacteria package these proteins into inclusions bodies which can be isolated, denatured and refolded at specific conditions to obtain a higher yield. The refolding conditions can vary, but aim to stabilize the protein and allow enough time and denaturing for the proper conformation to dominate. It is important to take into consideration salt concentration, pH, denaturing compounds, temperature and time when using chemical refolding techniques. Depending on the amino acids present, some proteins refold better under specific conditions than others. BMP-2 is known, and has been confirmed by our lab, to refold well under specific chemical refolding conditions while Nodal remains elusive. Research completed by Allendoph et al. revealed that while wild type activin does not refold well, chemically refolded chimeras of BMP-2 and activin retain activin-like signaling while producing refolding yields similar to BMP-2 (Allendorph). In this project, BMP-2 and Nodal were recombined forming chimeras that successfully refolded. Several chimeras were proven to exhibit Nodal-like signaling properties. Our lab looks forward to further analyzing these chimeras in in vitro settings in hopes of identifying novel functionality.

This Thesis, in part, is being prepared for publication of the material as it may appear as Blackler, Alissa N., Allendorph, George P., Choe, Senyon, Gray, Peter 2010. The thesis author will be the primary investigator and author of this paper.

Materials and Methods:

BMP-2/Nodal Ligand Expression and Inclusion Body Purification

BMP-2/Nodal ligands were expressed and inclusion bodies were purified as previously described with the following modifications (Groppe 1998). The 12 BMP-2/ Nodal segments were ordered from Integrated DNA Technologies, ligated to form the 64 constructs, and cloned into pET21a expression vectors. They were transformed into BL21 cells (Invitrogen) and allowed to multiply in terrific broth (EMD) at 37˚C until they reached an optical density of 0.8. 50mM Isoporpyl Beta-D-1-thiogalactopyranoside (IPTG) was used to induce expression. Four hours after cells were induced, a 5 minute spin at 4500xg allowed for harvesting the cell pellet. To isolate the inclusion bodies containing the BMP-2/Nodal constructs, the whole cell pellets were re-suspended in 5ml/1g with 50mM Tris-HCl pH 8.0 and 40mM EDTA. .2mM phenylmethanesulphonylfluoride (PMSF) was added before 3.3mg/ml of Lysozyme. The mixture was stirred for 10 minutes at 4˚C before 3-4 1 minute rounds of sonication. Next, .2mM PMSF and 0.1% Triton X-100 was added. The mixture was then centrifuged at 4500xg for 30 minutes at 4˚C. Two washes were completed by, re-suspending the pellet in 10mM TRIS-HCl pH 8.0, 1mM EDTA pH 8.0, and 1mM DTT using 2/3 volume used to re-suspend whole cell pellets. Following re-suspension, the samples were spun for 30 minutes at 4,500xg and 4˚C. The final pellet was re-suspended in 10mM TRIS-HCL pH 8.0, 1mM EDTA pH 8.0 and 1mM DTT at 2ml/ 1L of expression volume. Bradford

assays were used to determine the concentration of the isolated inclusion bodies

BMP-2/Nodal Refolding and Purification

BMP-2/Nodal chimeras were refolded and purified as previously described with the following modifications (Groppe 1998). Inclusion bodies were resuspended in 2.5mg/ml of a denaturing buffer consisting of 6M Guanidine-HCl, 50mM Tris pH 8.0, 2mM EDTA and 1mM DTT. They rotated at room temperature overnight. After incubation, samples were centrifuged at 16,000xg for 3 minutes and the supernatant was diluted into refolding buffer (100ml refoldings at 50mg/L). Refolding buffer consisted of 15˚C pre-chilled 50mM Tris-HC,l 2mM EDTA pH 8.0, 33mM CHAPS (1.8%w/v), 1.25 NaCl, 2mM reduced glutathione, and 1mM oxidized glutathion. The BMP-2/Nodal constructs were incubated for 120 hours at 15˚C. The refolded BMP-2/Nodal ligands were diluted 20 fold into 6M Urea, 2mM EDTA pH 8.0, and 50mM TRIS-HCl and concentrated down to approximately 50ml using a tangential flow concentrator. The solution containing the refolded protein was applied to a HiTrap Heparin column (GE Healthcare) and eluted with High Performance Liquid Chromatography (HPLC) using a sodium chloride gradient, 6M Urea, 50mM Tris-HCl pH 8.0, and 2mM EDTA pH 8.0. 15% SDS PAGE gels were visualized using Coomassie Brilliant Blue stain to verify dimer within the heparin column elutions. Promising samples were run through HPLC with a C4 reverse phase column (GraceVydac) and eluted with an acetonitrile gradient containing .1% trifluoracetic acid. Fractions with dimer formation were flash frozen using liquid nitrogen and put under a vacuum for lyophilization. 10mM sodium acetate

pH 4.0 was used to reconstitute lyophilized protein. Dimer formation was verified using SDS-PAGE as mentioned previously.

SMAD 2 Phosphorylation

HEK 293T cells were plated on 6-well plates at a density of 2 × 105cells/well. 24 hours after plating, cells were transfected with 2 μg of DNA (either empty vector or Cripto-Flag) using Perfectin. 24 hours after transfection, cells were serum-starved overnight prior to treatment (1 ml/well DMEM + P/S + gln). Cells were left untreated or treated for 30 min with 30nM Nodal (obtained from R & D Systems) or BMP-2/Nodal chimeras. Cells were harvested by adding 150 μl of ice-cold radioimmune precipitation buffer (50 mMTris-HCl, pH 7.4, 150 mM NaCl, 1% Nonidet P-40, 0.5% deoxycholate, 0.1% SDS) supplemented with 50 mM β-glycerol phosphate, 20 mM NaF, and standard protease inhibitors. Fifty μl of 4× SDS-PAGE loading buffer were then added to each sample, and the proteins were separated by SDS-PAGE and blotted to nitrocellulose. Blots were treated with anti-phospho-Smad2 or anti-Smad2/3 antibodies, followed by anti-rabbit IgG antibody conjugated to horseradish peroxidase, and bands were detected using enhanced chemiluminescence.

This Thesis, in part, is being prepared for publication of the material as it may appear as Blackler, Alissa N., Allendorph, George P., Choe, Senyon, Gray, Peter 2010. The thesis author will be the primary investigator and author of this paper.

Results:

Synthesis of BMP-2/Nodal Chimera

In order to recombine BMP-2 and Nodal, we aligned their sequences and looked for similar sections that did not interrupt theoretical structural motifs to subdivide the proteins. In order to create an overlapping PCR, we substituted the 77th amino acid in Nodal from alanine to a valine, and the 95th amino acid from leucine to valine. Both proteins were divided into six sections and ligated to create sixty four unique constructs. Each construct was inserted into pet21A vectors and propagated in Nova Blue cells. Once the correct construct was isolated, it was transformed into BL21 cells and expressed for four hours.

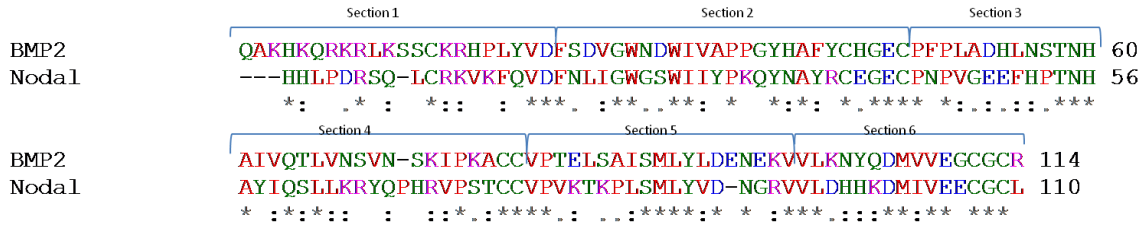

Figure 6: Sequence alignment of BMP-2 and Nodal. Sections are broken into the fragments used to construct the 64 chimeras.

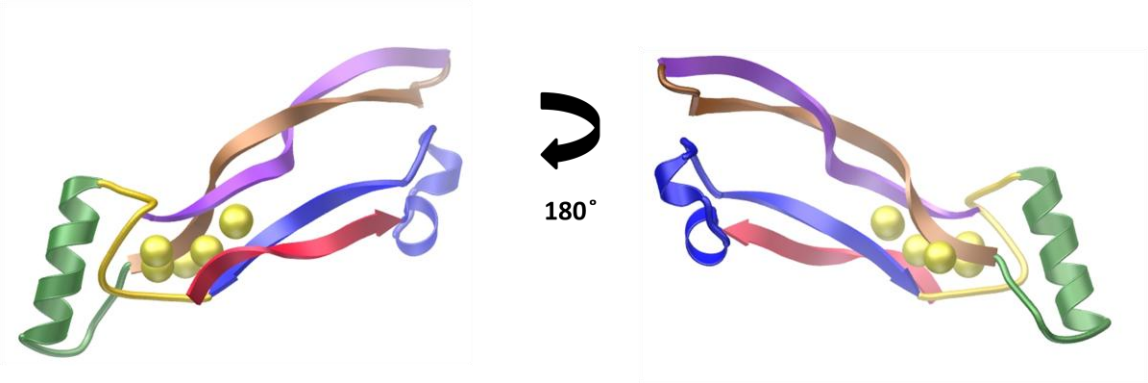

Figure 7: Three dimensional configuration of BMP-2/Nodal chimera. Different colors represent each of the six sections.

Inclusion bodies were isolated, purified and subjected to refolding conditions. A tangential flow concentrator was used to lower the NaCl concentration in the refolded protein. The constructs were then subjected to a heparin column and eluted with a NaCl gradient. Resulting eluted protein was run on a 15% SDS PAGE gel. Peaks that displayed dimer formation on the gel were run over reverse phase chromatography on a C4 column and eluted with acetonitrile. The eluted protein was lyophilized and run on a 15% SDS PAGE gel to confirm dimer formation.

Table 1: Summary of the amount of protein obtained after reverse phase chromatography. All constructs were subjected to 100ml refolding conditions at 50mg/L. The numbers describing each construct refer to the section pictured in figure 1. The "n" or "b" specify whether that section originated from Nodal or BMP-2. Constructs that produced dimer are indicated in red with the amount of µg obtained after lyophilization. VP indicates visible precipitation when sample was subjected to refolding conditions. BA indicates that heparin bound aggregated protein was the overwhelming product of the refolding. M indicates that the predominant product was monomer.

BMP-2/Nodal Construct	µg of lyophilized protein	BMP-2/Nodal Construct	µg of lyophilized protein
1n2n3n4n5n6n	VP	1b2b3b4b5b6b	267µg
1n2n3n4n5n6b	VP	1b2b3b4b5b6n	68µg
1n2n3n4n5b6n	BA	1b2b3b4b5n6b	13µg
1n2n3n4b5n6n	M	1b2b3b4n5b6b	320µg
1n2n3b4n5n6n	VP	1b2b3n4b5b6b	45µg
1n2b3n4n5n6n	BA	1b2n3b4b5b6b	50µg
1n2b3b4n5n6n	BA	1b2n3n4b5b6b	34µg
1n2b3n4b5n6n	VP	1b2n3b4n5b6b	VP
1n2b3n4n5b6n	M/BA	1b2n3b4b5n6b	BA
1n2b3n4n5n6b	BA	1b2n3b4b5b6n	86µg
1n2n3b4b5n6n	VP/M	1b2b3n4n5b6b	68µg
1n2n3b4n5b6n	M	1b2b3n4b5n6b	105µg
1n2n3b4n5n6b	VP	1b2b3n4b5b6n	55µg
1n2n3n4b5b6n	M	1b2b3b4n5n6b	10µg
1n2n3n4b5n6b	VP/M	1b2b3b4n5b6n	86µg
1n2n3n4n5b6b	M	1b2b3b4b5n6n	M
1n2b3b4b5n6n	M	1b2n3n4n5b6b	46µg
1n2b3b4n5b6n	M	1b2n3n4b5n6b	BA
1n2b3n4b5b6n	M	1b2n3b4n5n6b	M
1n2n3b4b5b6n	M	1b2b3n4n5n6b	25µg
1n2b3b4n5n6b	VP	1b2n3n4b5b6n	20µg
1n2b3n4b5n6b	VP	1b2n3b4n5b6n	15µg
1n2n3b4b5n6b	VP/BA	1b2b3n4n5b6n	259µg
1n2b3n4n5b6b	BA	1b2n3b4b5n6n	BA
1n2n3b4n5b6b	38µg VP	1b2b3n4b5n6n	M
1n2n3n4b5b6b	BA	1b2b3b4n5n6n	M
1n2b3b4b5b6n	BA	1b2n3n4n5n6b	BA
1n2b3b4b5n6b	VP	1b2n3n4n5b6n	34µg
1n2b3b4n5b6b	BA	1b2n3n4b5n6n	BA
1n2b3n4b5b6b	VP	1b2n3b4n5n6n	BA
1n2n3b4b5b6b	M	1b2b3n4n5n6n	44µg
1n2b3b4b5b6b	75µg	1b2n3n4n5n6n	20µg

Constructs beginning with the Nodal segment first were far less likely to produce any dimer. Their formation of visual precipitation during refolding incubation lead to aggregation, a lack of dimer, and low protein binding to the heparin column. In constructs beginning with the BMP-2 segment first, there was a higher incidence of dimer formation. Constructs with more BMP-2 segments proved more likely to form dimer.

Refolding Results for 1b2n3n4n5b6n construct:

Construct 1b2n3n4n5b6n was composed of mostly Nodal segments and resulted in dimer formation. The heparin affinity chromatogram shows three visible peaks between 40 and 70 minutes. The SDS PAGE gel of the resulting peaks shows dimer formation and increased aggregate present as time continued throughout the run. Each collected peak was subjected to purification through a reverse phase C4 column, resulting in clean dimer peaks shown in the SDS PAGE gel.

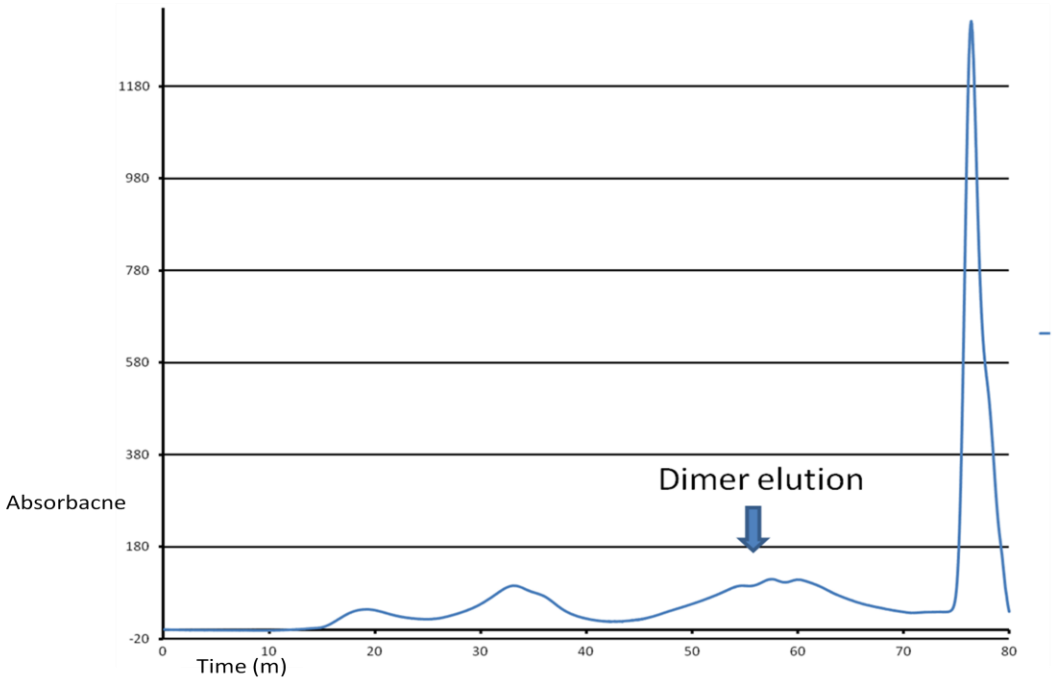

Figure 8: Heparin affinity chromatography run of Bmp-2/Nodal construct 1b2n3n4n5b6n. A shallow NaCl gradient was used to elute the dimer which comes off between 50 and 70 minutes.

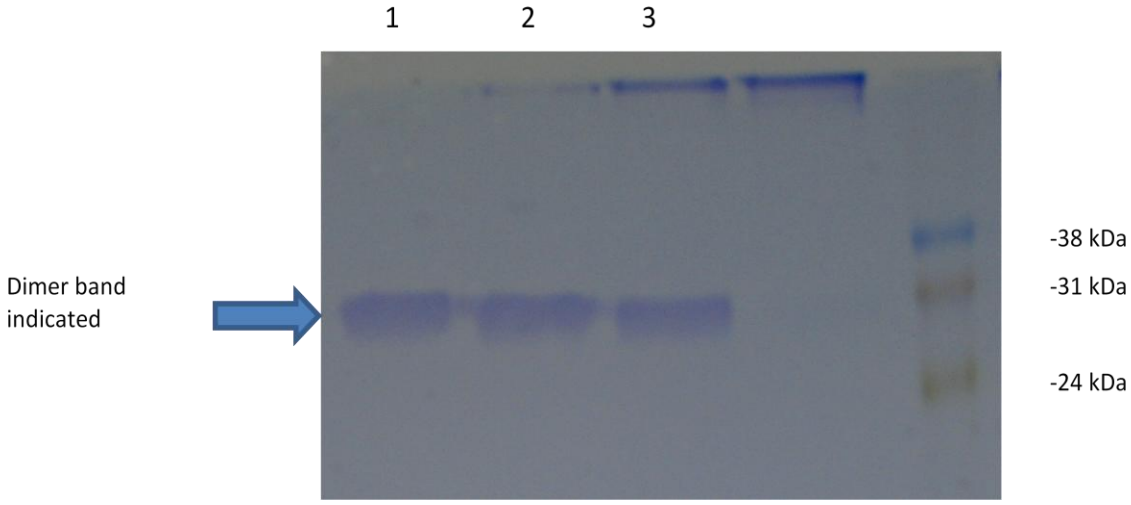

Figure 9: SDS-PAGE gel of elutions from heparin run of BMP-2/Nodal construct 1b2n3n4n5b6n. Lane 1 contains the elution from 47.3-52.4 minutes. Lane 2 contains the elution from 52.4-55.7 minutes. Lane 3 contains the elution from 55.7-59 minutes. Dimer bands migrate around 30kDa when subjected to non-reducing conditions. The theoretical molecular weight for a dimer consisting of all BMP-2 segments is 25,809Da while a dimer consisting of all Nodal segments is 25,647Da.

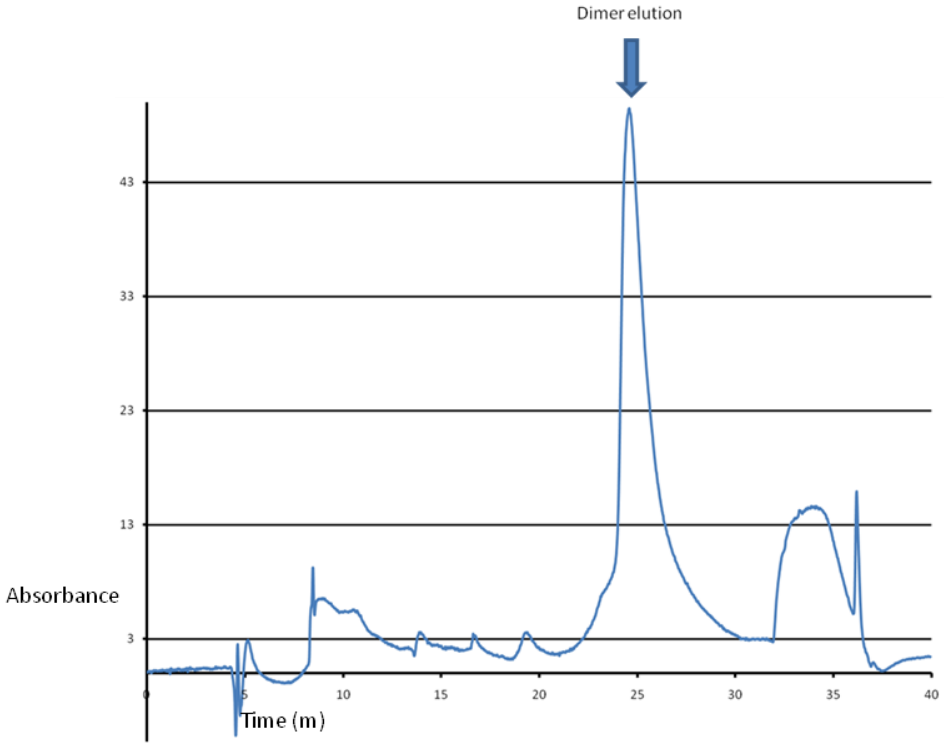

Figure 10: Reverse Phase C4 Chromatography run of BMP-2/Nodal construct 1b2n3n4n5b6n elution 47.3-52.4 of heparin run. Approximately 81µg of protein was run.

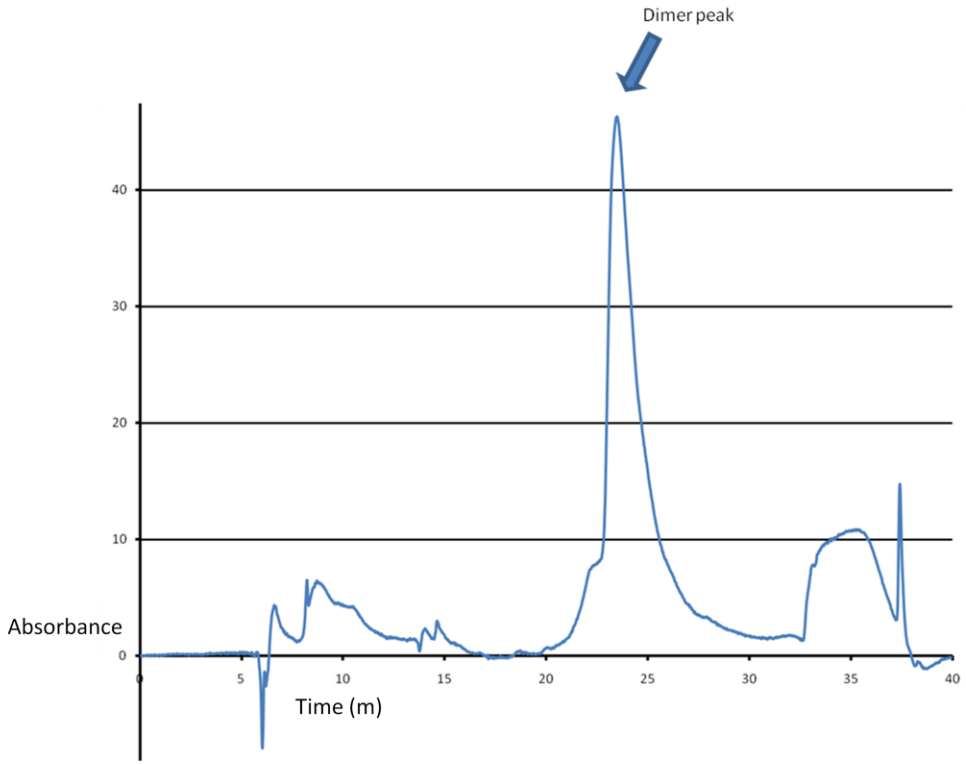

Figure 11: Reverse Phase C4 chromatography run of BMP-2/Nodal construct 1b2n3n4n5b6n elution 52.4-55.7 minutes of heparin run. Approximately 90µg of protein was loaded.

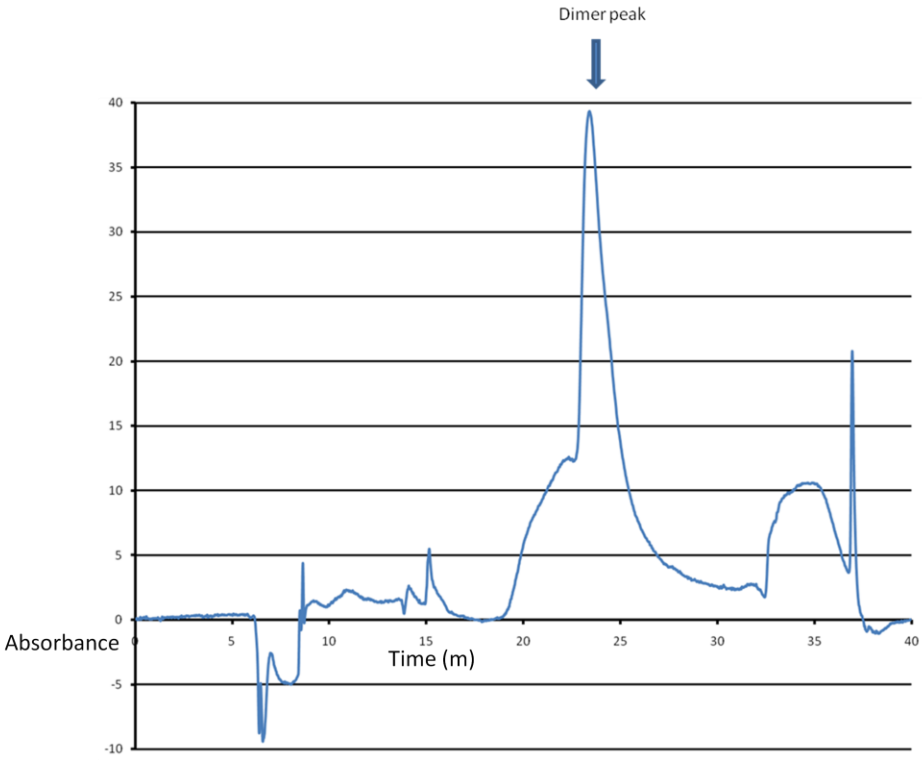

Figure 12: Reverse Phase C4 chromatography run of BMP-2/Nodal construct 1b2n3n4n5b6n elution 55.7-59.0 minutes of heparin run. Approximately 100 µg of protein was loaded.

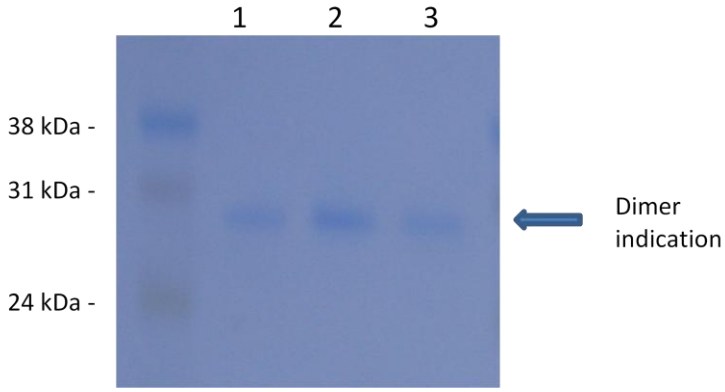

Figure 13: SDS-PAGE gel of reverse phase chromatography runs of BMP-2/Nodal 1b2n3n4n5b6n construct. Lane 1 contains elution 24.2-25.2 minutes from C4 run of heparin elution 47.3-52.4. Lane 2 contains elution 23.1-24.1 minutes from C4 run of heparin elution 52.4-55.7. Lane 3 contains elution 23.1-23.9 minutes from C4 run of heparin elution 55.7-59.0.

Refolding Results for 1b2b3n4n5n6n construct:

Construct 1b2b3n4n5n6n was composed of mostly Nodal segments and resulted in dimer formation. The heparin affinity chromatogram exhibits two visible peaks between 40 and 70 minutes. The SDS PAGE gel of the resulting peaks shows dimer formation as well as other sized products within the elutions. When subjected to reverse phase C4 chromatography, both heparin elutions resulted in two separate peaks, the smaller of which resulted in clean dimer as revealed by the SDS PAGE gel.

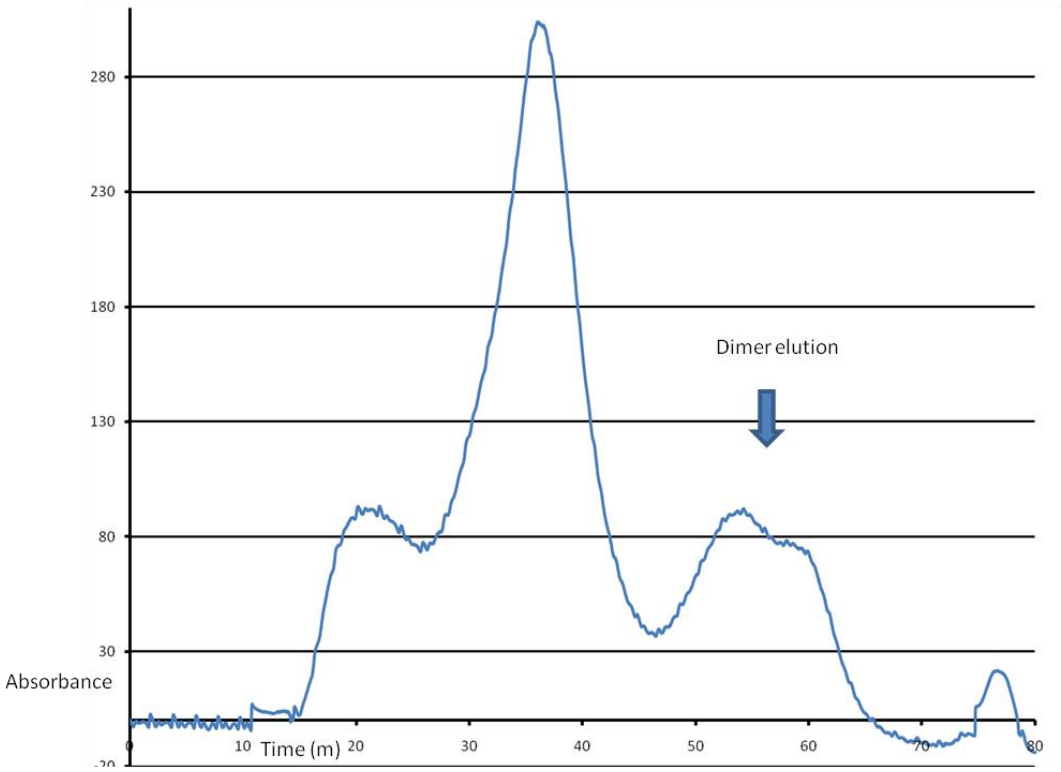

Figure 14: Heparin affinity chromatography run of BMP-2/Nodal construct 1b2b3n4n5n6n. A shallow NaCl gradient was used to elute the dimer which comes off between 50 and 70 minutes.

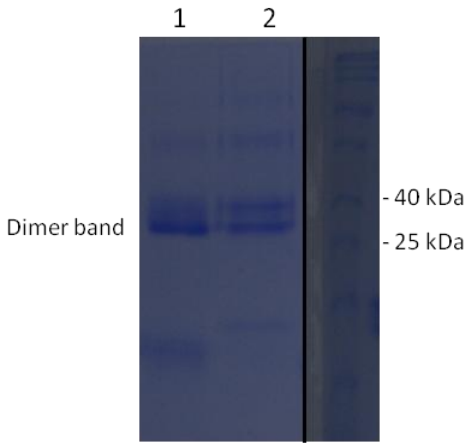

Figure 15: SDS-PAGE gel of Heparin affinity chromatograhy run of BMP-2/Nodal construct 1b2b3n4n5n6n. Lane 1 contains elution 47.6-59.8 minutes. Lane 2 contains elution 59.8-64.0 minutes.

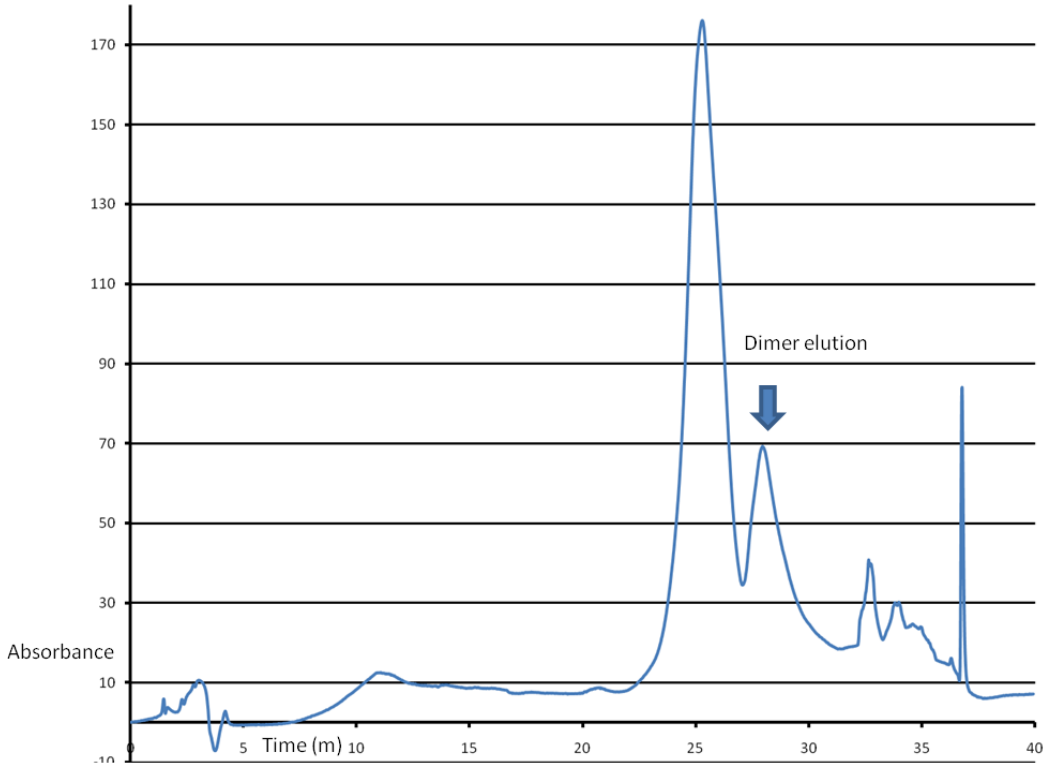

Figure 16: Representative reverse Phase C4 chromatography run for both peaks between 50-70 minutes. This chromatogram is BMP-2/Nodal construct 1b2b3n4n5n6n elution 47.6-59.8 minutes of heparin run. Approximately 260 µg of protein was loaded.

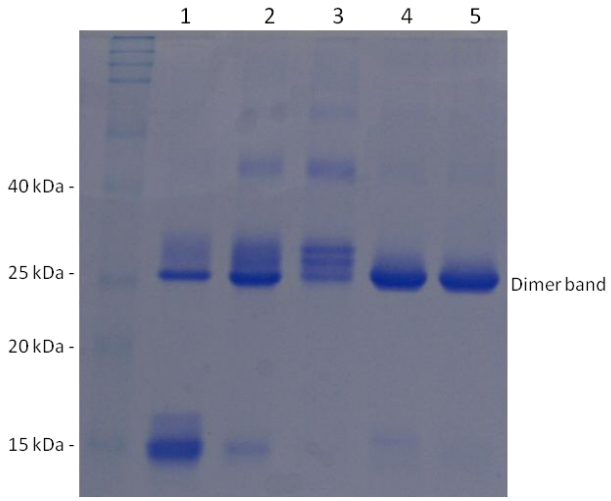

Figure 17: SDS-PAGE gel of reverse phase chromatography runs of BMP-2/Nodal construct 1b2b3n4n5n6n from heparin elution 47.6-59.8 minutes. Lane 1 contains elution 23.9-25.0 minutes. Lane 2 contains elution 25-26 minutes. Lane 3 contains elution 26-27.1 minutes. Lane 4 contains elution 27.4-28.4 minutes. Lane 5 contains elution 28.4-29.5 minutes.

Refolding Results for typical BMP-2 refolding:

BMP-2 has been documented as producing dimer under chemical refolding conditions. The heparin affinity displays a clean dimer peak between 50 and 70 minutes. The SDS PAGE gel shows that the peak collected between 56 and 62 minutes is clean dimer. The subsequent reverse phase C4 chromatography run and SDS PAGE gel confirm the presence of dimer.

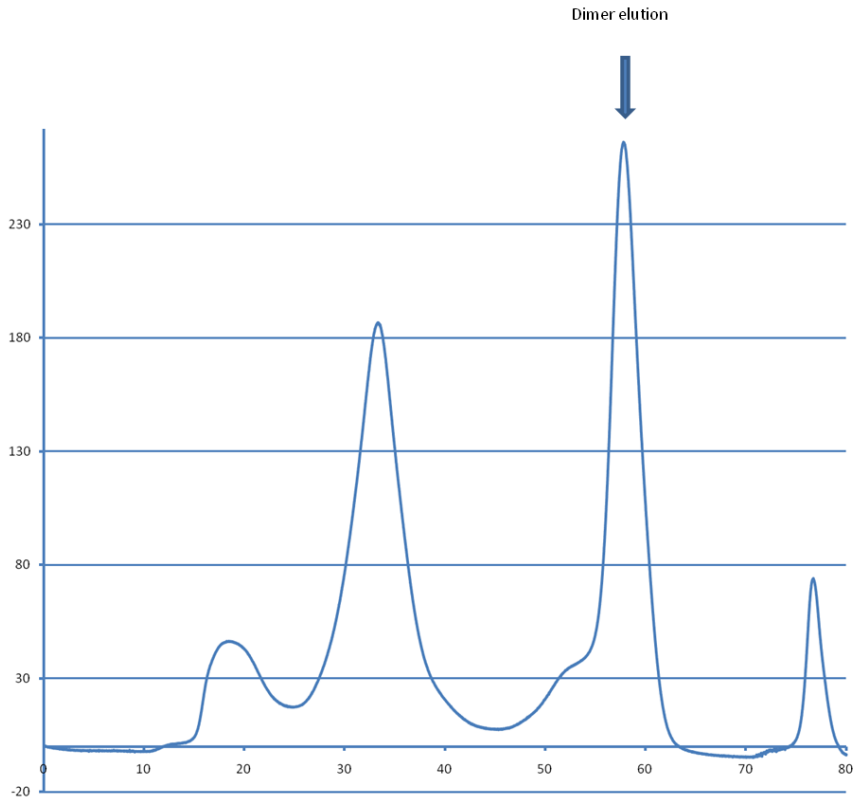

Figure 18: Heparin affinity chromatography run of BMP-2 1b2b3b4b5b6b. A shallow NaCl gradient was used to elute the dimer which comes off between 50 and 70 minutes. The size of the dimer peak is notable when compared to the earlier monomer peak.

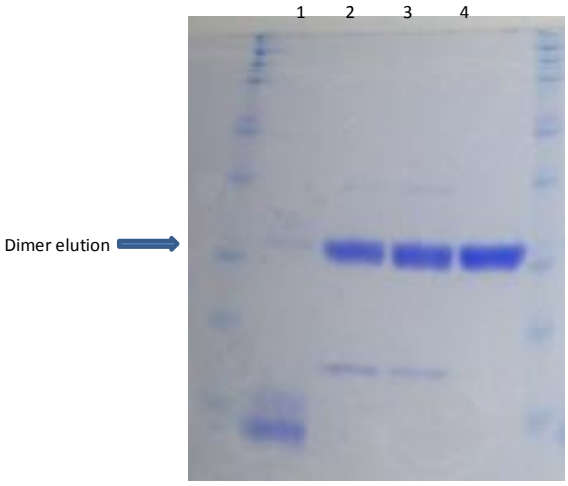

Figure 19: SDS-PAGE gel of Heparin affinity chromatography run of BMP-2 construct 1b2b3b4b5b6b. Lane 1 contains elution 28-39 minutes. Lane 2 contains elution 50-54 minutes. Lane 3 contains elution 54-56 minutes. Lane 4 contains elution 56-62 minutes.

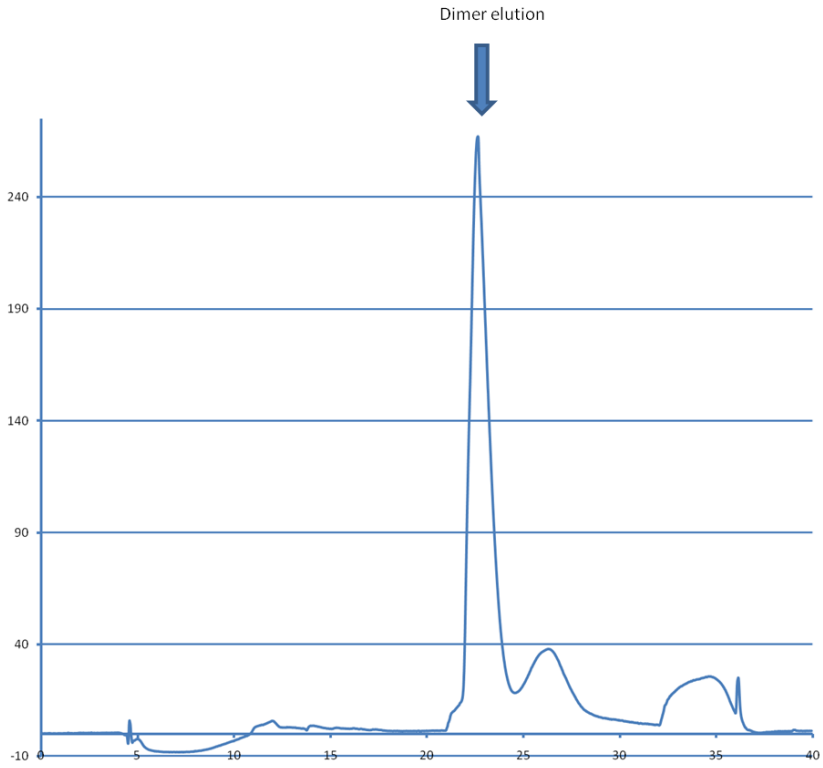

Figure 20: Reverse Phase C4 chromatography run of BMP-2 construct 1b2b3b4b5b6b elution 58-62 minutes of heparin run. Approximately 300 µg of protein was loaded.

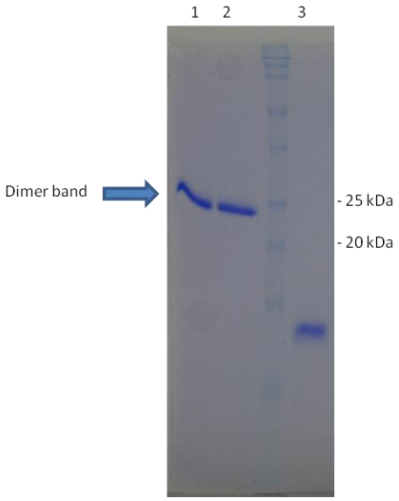

Figure 21: SDS-PAGE gel of reverse phase chromatography runs of BMP-2 construct 1b2b3b4b5b6b. Lane 1 contains elution 22.0-22.7 minutes from C4 run of heparin elution 58-62 minutes. Lane 2 contains elution 22.7-24.0 minutes from C4 run of heparin elution 58-62 minutes. Lane 3 contains the reduced form of elution 22.7-24.0 minutes from C4 run of heparin elution 58-62 minutes.

Representative Refolding resulting in aggregate formation:

This chromatogram represents the chimeras that resulted in predominant formation of aggregate that binds to the heparin column and elutes once the sodium chloride concentration reaches 1M.

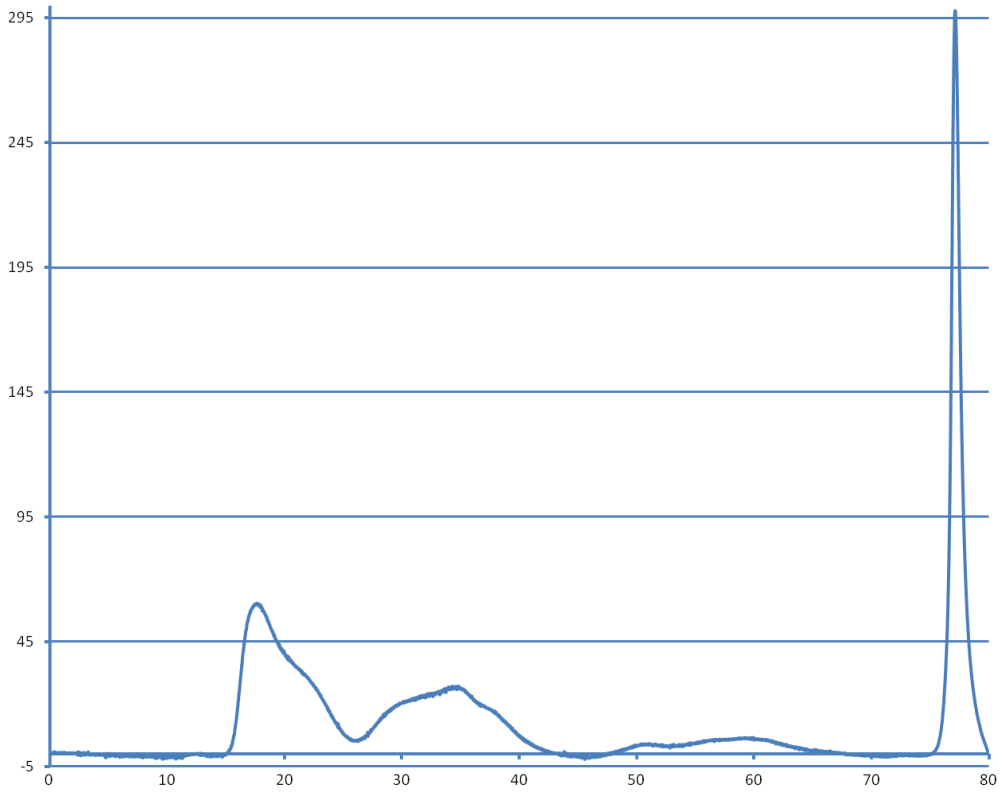

Figure 22: Representative chromatogram of a construct that binds mostly as aggregate during the heparin affinity chromatography. This particular construct was BMP-2/Nodal 1n2n3n4n5b6n.

Representative refolding resulting in monomer formation:

This chromatogram represents chimeras that predominantly result in monomer formation. Most of the protein elutes during the first 40 minutes.

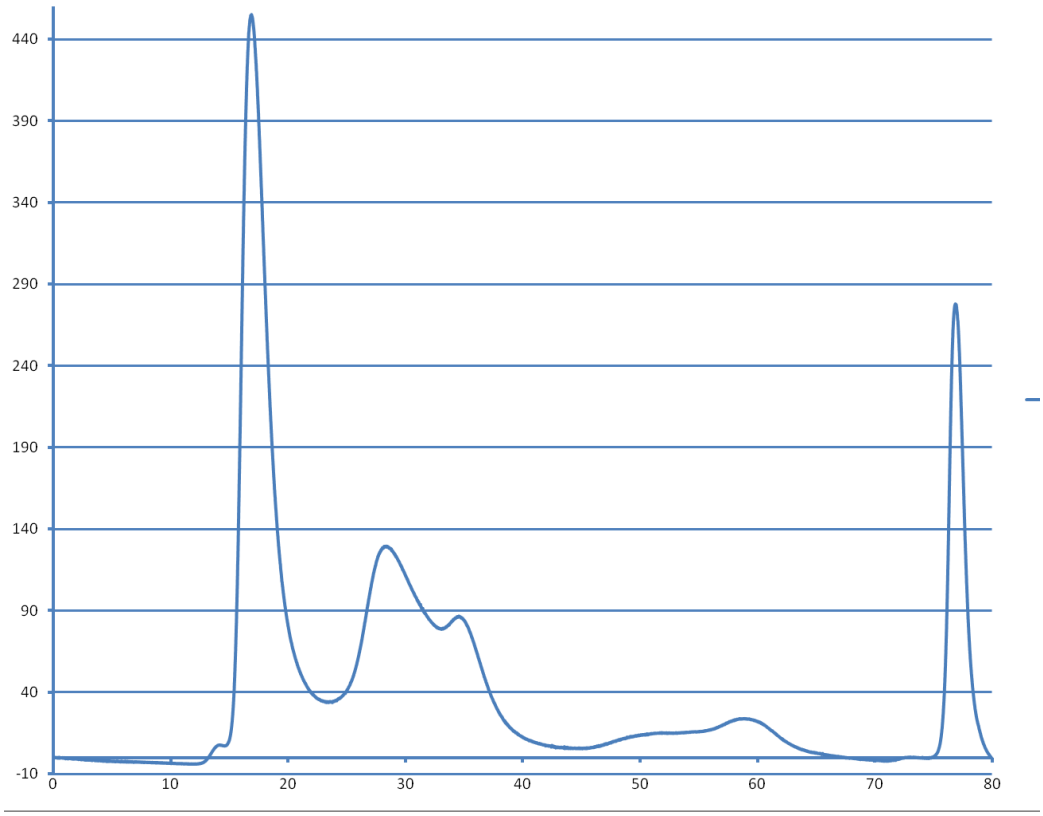

Figure 23: Representative chromatogram of a construct that binds mostly as monomer during the heparin affinity chromatography. This particular construct was BMP-2/Nodal 1n2n3n4b5n6n.

Functional Testing of BMP-2/Nodal Chimeras

After chimeras were refolded, purified and lyophilized, the three constructs with four Nodal segments and one construct with three Nodal segments were tested for Nodal-like signaling. Nodal is known to phosphorylate Smad-2 in a Cripto-dependent manner. Using HEK 293 T cells, we compared mammalian derived Nodal signaling to our chimeras in the presence and absence of Cripto. Using anti-phospho-Smad-2, the Western blot indicates that wild type (wt) Nodal, along with constructs 1b2n3n4n5n6n, 1b2n3n4n5b6n, and 1b2n3n4n5b6b lack signaling without Cripto. Strong bands in the presence of Cripto for these molecules show Ciptro-dependent Smad-2 phosphorylation

and suggest Nodal-like signaling. Construct 1b2b3n4n5n6n did not show Smad-2 phosphorylation in the presence or absence of Cripto.

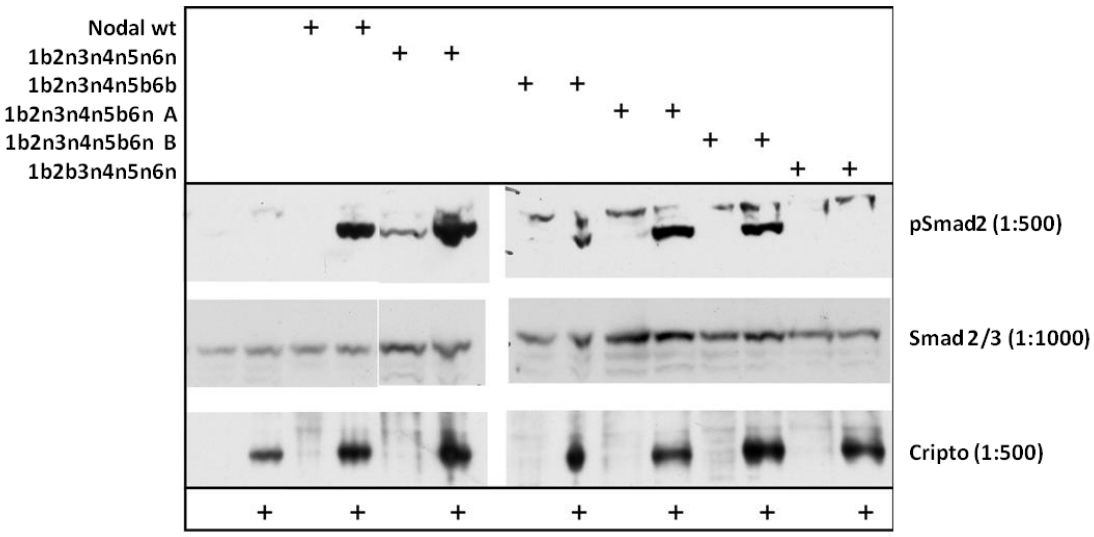

Figure 24: Cripto-dependence of Smad-2 phosphorylation. HEK 293 T cells were transfected with empty vector or Cripto and treated with indicated Nodal and BMP-2 Nodal chimeras. The resulting cell lysates were subjected to Western blotting using phospho-Smad-2, Smad2/3, or Cripto antibodies as described in "Materials and Methods".

This Thesis, in part, is being prepared for publication of the material as it may appear as Blackler, Alissa N., Allendorph, George P., Choe, Senyon, Gray, Peter 2010. The thesis author will be the primary investigator and author of this paper.

Discussion:

The TGF-β superfamily consists of over thirty ligands critical in tissue patterning and generation, early embryo development and pluripotency maintenance. Pivotal to understanding the roles each ligand has in living systems and their therapeutic potential, large quantities of these ligands must be produced to continue research. While BMP-2, BMP-3, BMP-4 BMP-6, TGF-βI, TGF-βII, TGF-βIII, GDF-5, GDF-6 and GDF-7 have been refolded chemically to produce sufficient amounts of properly refolded protein, many of the most interesting TGF-β ligands have not yet been successfully refolded from *E. Coli* (Long et al. 2005, Klosch et al. 2005, Schlunegger et al. 1992). Nodal, a ligand essential in stem cell differentiation, axis formation and necessary during the first stages of life has not been successfully refolded. Increasing availability of Nodal through chemical refolding would help understanding of Nodal/ receptor complex formation and downstream signaling events as well as its function in later stages of development. Using methods modified from Allendorph et al., we were successful in creating chimeras of BMP-2 and Nodal possessing Nodal-like signaling motifs (Allendorph).

To better understand the structural importance of each segment, I analyzed them based on each construct's refolding capability. As seen in Table 1, only two chimeras beginning with a Nodal segment in the first position produced properly folded ligand. Contrastingly, twenty chimeras beginning with a BMP-2 segment in the first position produced properly refolded protein. Also, thirteen chimeras with a Nodal segment in the first position visibly aggregated during refolding as opposed to one chimera with a BMP-2 segment in the first position. Constructs that visibly precipitated were refolded using

lower protein concentrations. Unfortunately, reducing the concentration from 50mg/L to 25mg/L did not aid in yield. These results suggest that the amino terminus of the TGF-β ligands is important in proper dimer formation and chemical refolding. One obvious difference that might attribute to the difference in refolding results in the 1b segment compared to the 1n segment is that 1n has four less basic residues compared to the first segment of BMP-2. Moreover, basic residues allow binding to the heparin column, possibly accounting for some of the differences in binding when comparing 1n constructs to 1b constructs. The importance of the first segment in regards to refolding is further illustrated in Allendorph et al (Allendorph 2010). In their work, Allendorph was able to efficiently chemically refold a chimera consisting of one BMP-2 segment in the first position and activin segments in position two through six (Allendorph 2010). This data contrasts wild type activin's inability to chemically refold. My data combined with findings in Allendorph et al further reinforce the importance of the amino terminus in proper chemical refolding.

Table 1 also reveals that constructs incorporating more BMP-2 segments than Nodal segments form more refoldable ligand than constructs containing more Nodal than BMP-2 segments. This result can easily be predicted based on prior knowledge of BMP-2 and Nodal refolding efficiencies.

In order to compare our chimera's signaling capabilities to Nodal, we tested for Smad-2 phosphorylation, a known downstream signaling event initiated by Nodal. As pictured in Figure 24, constructs 1b2n3n4n5n6n, 1b2n3n4n5b6b, and 1b2n3n4n5b6n show Cripto-dependent Smad-2 phosphorylation similar to that of wild type Nodal. Construct 1b2b3n4n5n6n did not exhibit phosphorylation of Smad-2. While all tested

constructs share the third and fourth nodal segment, only constructs displaying Smad-2 phosphorylation possess the 2n section. The construct that did not show Smad-2 phosphorylation incorporates the 2b section. This finding suggests that the second, third and fourth sections are important to Nodal signaling, and that signaling without the 2n section may not be possible. The 2n section appears to be necessary for Cripto-dependent ligand signaling. Based on what we know about ligand complex formation in combination with our results, the 2n section is most likely responsible for Cripto binding. However, the lack of signaling in the presence of the 2b section may result in inhibition of Type-I or Type-II receptor binding. In order to test the importance and necessity of the 2n segment, we should try testing 1b2n3b4b5b6b and 1b2b3n4n5b6b. This information would also give us insight into the importance of the 3n and 4n section.

In the future, we hope to subject more of our chimeras to assays that asses Nodal-like signaling capability. Constructs that show promising Smad activation will be subjected to assays that test endogenous pathways using NCCIT cells which naturally over-express Cripto. Additionally, we will use Bia Core affinity assays to determine binding affinity and complex formation by assessing which portions of the complexes can associate independently. Luciferase assays will be useful to test for potency of signaling strength by comparing BMP-2/Nodal constructs to wild type Nodal.

Many cancers are correlated with over-expression of Cripto, leading researchers to investigate Cripto associated cancer therapies (Adkins et al 2003, Xing et al.2004). Our potential to isolate, and possibly impart on other TGF-β ligands, the section of Nodal responsible for Cripto-dependence allows the potential to target cancers associated with endogenous Cripto over-expression. We can test our constructs, or attempt to create a

new Cripto dependent BMP-2 to target cancer cells that over-express Cripto to activate Smad-1 induced apoptosis. Research has indicated that some cancers, for example prostate cancer, show decreased cell motility in response to increased Smad-1 activation (Craft et al 2007). Also, TGF-β1 has been linked to growth suppression of many cell types including lymphoid and epithelial cells in humans and plays a role in suppressing primary tumorgenesis (Roberts et al. 2003, Pardali et al. 2007). It may be possible to recombine Nodal and TGF-β1 to create a Cripto-dependent TGF-β1 with the ability to specifically target cancer cells over-expressing Cripto and elicit a tumor suppressing signal cascade. Another potential use for our chimeras may be recombining one of our Cripto-dependent ligands with a signal peptide that can elicit an immune response against Cripto over-expressing tumors.

Allendorph was able to produce BMP-2/ activin chimeras with higher affinity to receptors than either BMP-2 or activin alone. Some of his chimeras also show greater Smad activation than wild type activn and wild type BMP-2. Based on these results, it would be interesting to make a chimera consisting of BMP-2, activin and Nodal, possibly rendering a cripto independent Nodal-like ligand, or a Noldal-like molecule that signals with amplified strength.

Constructs showcasing potentially useful functionality will be subjected to a refolding screening to optimize the conditions. Using arginine, or urea, or adjusting the salt concentration are a few variables we could attempt to refine and better suit BMP-2/Nodal chimeras. Furthermore, we could alter the constructs by substituting pivotal residues in Nodal segments that might aid in refolding. Allendorph was able to produce comparable protein yields to chemically refolded BMP-2 with his chimera consisting of a

BMP-2 segment in position one and activin segments in position two through six (Allendorph et al). Based on Allendorph's success and the similarity in signaling between Nodal and activin, we could produce a 1b2n3n4n5n6n chimera and attempt minimal substitutions of activin (or other refoldable TGF-β ligands) origin in the Nodal segments. This would hopefully produce better chemical refolding without significantly deviating from Nodal structure. It could potentially help to understand the significance of individual residues and sections in refolding, paving the way for other non-refoldable TGF-β ligands.

The information obtained from these experiments has lead to a better understanding of the importance of different segments in Nodal signaling and TGF-β ligand refolding.

This Thesis, in part, is being prepared for publication of the material as it may appear as Blackler, Alissa N., Allendorph, George P., Choe, Senyon, Gray, Peter 2010. The thesis author will be the primary investigator and author of this paper.

References:

1. Adkins, HB. Bianco C., Schiffer SG. Et al: 2003.Antibody blockade of the Cripto CFC domain suppresses tumor cell growth in vivo. J. Clin. Invest. 112(4): 575-578.

2. Allendorph, George. (2010). Design of TGF-β ligands with Diversified Functionality. Manuscript submitted for publication.

3. Chen C., Shen M.M. 2004. Two modes by which Lefty proteins inhibit nodal signaling. Curr. Biol. 14: 618-624.

4. Conlon F.L., Lyons K.M., Takausu N., Barth K.S. Kispert A., Herrmann B., and Robertson E.J. 1994. A primary requirement for nodal in the formation and maintenance of the primitive streak in the mouse. Development 120: 1919-1928

5. Craft, CS., Romero D., Vary CPH., Bergan RC. 2007. Endoglin inhibits prostate cancer motility via activation of the ALK-2-Smad1 pathway. Oncogene. 26: 7240-7250.

6. Daopin S., Piez K.A., Ogawa Y., and Davies D.R. 1992. Crystal structure of transforming growth factor-β2: An unusual fold for the superfamily. Science: 257: 369-373.

7. De Larco J.E. and Todaro G.J. 1978. Growth Factors from murine sarcoma virus-transformed cells. Proc. Natl. Acad. Sci. 75: 4001-4005.

8. Derynck, Rik, and Miyazono, Kohei. The TGF-β Family. New York: Cold Spring Harbor Laboratory Press, 2008.

9. Geiger M., Li R.H., and Friess W. 2003. Collagen sponges for bone regeneration with rhBMP-2. Advanced Drug Delivery Review. 55: 1613-1629.

10. Groppe J., Rumpel K., Economides A., Stahl N., Sebald W., and Affolter M. 1998. Biochemical and Biophysical Characterization of RefoldedDrosophilaDPP, a Homolog of Bone Morphogenetic Proteins 2 and 4. The Journal of Biological Chemistry. 273: 29052-29065.

11. Gu Z., Nomura M., Simpson B.B., Lei H., Feijen A., van den Eijnden-van Raaij J., Donahoe P.K., and Li E. 1998. The type I activin receptor ActRIB is required for egg cylinder organization and gastrulation in the mouse. Genes Dev. 12: 844-857.

12. Klosch, Burkhard., Furst, Wlater,. Kneidinger, Rudolf, Schuller, Monika, Rupp, Barbara, Banerjee, Asmita, and Reld, Heinz. Expression and Purification of Biologically Active Rat Bone Morphogenetic Protein-4 produced as Inclusion Bodies in Recombinant *Escherichia coli*. Biotechnology Letters. 27 (20): 1559-1564.

13. Long, Shinong, Lynn Truong, Bennett, Krista, Phillips, Andrew, Wong-Staal, Flossie, and Ma, Hongwen. 2005. Expression, purification, and renaturation of bone morphogentic protein-2 from *Escherichia coli*. Protein Expression and Purification. 46, (2): 374-378.

14. Mason A.J., Hayflick J.S., Ling N., Esch F., Ueno N., Ying S.Y., Guillemin R., Niall H., and Seeburg P.H. 1985. Complementary DNA sequences of ovarian follicular fluid inhibin show precursor structure and homology with transforming growth factor- β. Nature 318: 659-663.

15. Massague, J., Wotton, D., 2000. The EMBO Journal 19: 1745-1754

16. Mazerbourg S., Klein C., Roh J., Kaivo-Oha N., Mottershead D.G., Korchynskyi O., Ritvos O., and Hsueh A.J. 2004. Growth differentiation factor-9 signaling is mediated by the type I receptor, activin receptor-like kinase 5. Mol. Endocrinol. 18: 653-665.

17. McDonald, N.Q., and Hendrickson, W.A. (1993). A structural superfamily of growth factors containing a cystine knot motif. Cell 73, 421-424.

18. Michael M. Shen. 2003. Decrypting the role of crypto in tumorgenesis. J Clin Invest vol 112, (4): 500-502

19. Moore F.K., Otsuka F., and Shimasaki S. 2003. Molecularbasis of bone morphogenetic protein-15 signaling in granulose cells. J. Biol. Chem 267:2325-232

20. Moses H.L., Branum E.L., Prober J.A., and Robinson R.A. 1981. Transforming growth factor production by chemically transformed cells. Cancer Res. 41 2842-2848.

21. Pardali, Katerina., and Moustakas, Aristidis. 2007. Actions of TGF-β as tumor suppressor and pro-metastatic factor in human cancer. Biochimica et Biophysica Acta- Reviews on Cancer. 1775 (1): 21-62.

22. Roberts, Anita., Wakefiled, Lalage M., 2003. The two faces of transforming growth factor β in carcinogenesis. Proc Natl Acad Sci U S A.100 (15): 8621-8623. Doi: 10.1073/pnas.1633291100.

23. Schier A.F. 2003. Nodal signaling in vertebrate development. Annu. Rev. Cell. Dev. BIol. 19: 589-621.

24. Schier A.F. and Shen M.M. 2000. Nodal signaling in vertebrate development. Nature 403: 385-389.

25. Schlunegger M.P. and Grutter M.G. 1992. An unusual feature revealed by the crystal structure at 2.2Å resolution of human transforming growth factor-β2. Nature 358: 430-434.

26. Schlunegger, Michael P., Cerletti, Nico., Cox, David A., McMaster, Gary K., Schmitz, Albert., and Grutter, Markus G. 1992 Crystallization and preliminary X-ray analysis of recombinant human transforming growth factor β2. FEBS Letters, 303(1): 91-93.

27. Song J., Oh S.P., Schrewe H., Nomura M., Lei H., Okano M., Gridley T., and Li E. 1999. The type II activin receptors are essential for egg cylinder growth, gastrulation, and rostral head development in mice. Dev. Biol. 213: 157-169.

28. Tabibzadeh S. and Hemmati-Brivanlou A. 2006. Lefty at the crossroads of "stemness" and differentiative events. Stem Cells 24: 1998-2006.

29. Urist M.R. 1965. Bone formation by autoinduction. Science 150: 893.

30. Vale W., Rivier J., Vaughan J., McClintock R., Corrigan A., Woo W., Karr D., and Spiess J. 1986. Purification and characterization of an FSH releasing protein from porcine ovarian follicular fluid. Nature 321: 776-779.

31. Whitman M. and Mercola M. 2001. TGF-β superfamily signaling and left-right asymmetry. Sci. STKE 2001: RE1.

32. Xing PX., Hu, XF., Pietersz GA., Hosick HL., McKenzif IF. 2004. Cripto immunotherapy. Cancer Res. 64(11): 4018-4023.

33. Yu P.B., Beppu H., Kawai N., Li E., and Bloch K.D. 2005. Bone morphogenetic protein (BMP) type II receptor deletion reveals BMP ligand-specific gain of signaling in pulmonary artery smooth muscle cells. J. Biol. Chem. 280: 24443-24450.

34. Zhou X., Sasaki H., Lowe L., Hogan B.L., and Kuehn M.R. 1993. Nodal is a novel TGF-β-like gene expressed in the mouse node during gastrulation. Nature. 361: 543-547.